Dynamic light scattering as a probe of orientational dynamics in confined liquid crystals

A. Mertelj[1] and M. Čopič[1,2]
[1]*Jožef Stefan Institute, Jamova 39, 1001 Ljubljana, Slovenia*
[2]*Department of Physics, University of Ljubljana, 1000 Ljubljana, Slovenia*
(Received 13 September 1999)

The eigenmodes of director orientational fluctuations in nematic liquid crystals in confined geometries were studied both theoretically and experimentally by dynamic light-scattering tehnique. The fundamental mode of the orientational fluctuations shows a crossover from bulk behavior, dominated by bulk elastic constant K, to surface dominated one, in which the relaxation rate is determined by the ratio of surface anchoring strength W and viscosity η. The contribution of surface viscosity ζ is also significant when its characteristic length ζ/η becomes comparable to the size of the confined system. It was measured in nematic liquid crystal in cylindrical pores of polycarbonate (Nuclepore) membranes to be of the order of 10 nm.

PACS number(s): 61.30.Gd, 64.70.Md, 42.70.Df, 78.35.+c

I. INTRODUCTION

Pioneering work on dynamic light scattering (DLS) in bulk nematic liquid crystals has been done decades ago by Orsay Liquid Crystal Group [1,2]. It is a very convenient method to study the dynamics of orientational fluctuations of order parameter in different liquid crystalline phases. Using this method in bulk nematic liquid crystals one can measure elastic constants and viscosity coefficients.

Well-known turbid appearance of nematic liquid crystals is due to the scattering of light on thermally excited orientational fluctuations of nematic director. In the bulk the eigenmodes of these orientational fluctuations are exponentially relaxing plane waves with relaxation rates that depend on the viscoelastic properties of the material and on the wave vectors of the modes. The spectrum of the fluctuations is continuous, i.e., all wave vectors (within the continuum theory) are allowed, and the dispersion relation is typical of hydrodynamic modes with the relaxation rate proportional to the square of the wave vector. In DLS experiment one measures the relaxation rate of the eigenmode, which has the wave vector that is equal to the scattering vector. Typically in the experiment, one changes the scattering vector and therefore obtains the dispersion relation, i.e., relaxation rate vs wave vector. The results of the experiments are in good agreement with the continuum description of the nematic phase and its orientational fluctuations [3].

An important property of the liquid crystals is their interaction with surfaces [4]. In the case of the nematic liquid crystals one usually describes the interaction of the liquid crystal with the surface in terms of the preferred orientation of the nematic director at the surface, called easy direction, and the strength of the interaction. Formally speaking, the easy direction is the direction of the director at which the surface energy is minimal. The strength of the interaction is given by the quantity called anchoring strength, which tells what torque is needed to deviate the orientation of the director from the easy direction. In the continuum theory, one includes the presence of surface by boundary conditions. In the static case, the boundary conditions simply state that bulk torques (elastic torque, torques due to external fields) are balanced by the surface one. In the dynamic case the question arises whether also the viscous surface torque must be taken into account. The problem is similar to the case of ordinary fluids where one argues whether the fluid velocity at the boundaries is equal to zero or not [5]. If the orientation of the nematic director at the surface changes with time, one would expect a kind of dissipation connected with this motion. Usually this dissipation is described by introducing a surface orientational viscosity (see for example, Ref. [6]). This quantity has dimensions poise.m and strictly speaking, is not a viscosity but more something like a friction coefficient.

In this paper, we want to show how the surface properties affect the eigenmodes of orientational fluctuations and how they can be measured in the DLS experiments. Particular attention is given to the analysis of the scattering cross section. In Sec. II, we sketch how one calculates the eigenmodes of orientational fluctuations and their relaxation rates. We show how the eigenmode structure and the relaxation rates are affected by the surface properties. In Sec. III, light scattering on the eigenmodes of director orientational fluctuations is calculated and in Sec. IV experimental results and discussion are given.

II. EIGENMODES OF ORIENTATIONAL FLUCTUATIONS

In order to understand the results of the DLS experiments in confined nematic liquid crystals two things must be considered. First, the size of a typical cavity is not large compared to the wavelength of light and that must be considered in the analysis of scattering. And secondly, due to the confinement, the eigenmode structure of the orientational fluctuations in the nematic liquid crystal changes. Instead of plane waves and continuous spectrum as in the case of the bulk nematic liquid crystals, the eigenmodes are standing waves with shape depending on the geometry of the cavity, i.e., sinusoidal standing waves in the rectangular geometry [7], similar to Bessel and Neumann functions in the cylinders [8], to spherical Bessel functions in the droplets [9] etc. The allowed values of the wave vectors, or more precisely, of the eigenvalues are discrete and depend on the boundary conditions.

The eigenmodes of director orientational fluctuations are

exponentially relaxing modes with relaxation rate, which is in one elastic constant approximation given by the expression [3]

$$\frac{1}{\tau_N}=\frac{Kk_N^2}{\eta}, \tag{1}$$

where K is an effective Frank elastic constant and η an effective bulk viscosity. The eigenvalues k_N can be calculated from dynamic equation [9]

$$\nabla^2\mathbf{n}-(\mathbf{n}\cdot\nabla^2\mathbf{n})\mathbf{n}=\frac{\eta}{K}\frac{\partial}{\partial t}\mathbf{n}, \tag{2}$$

where $\mathbf{n}(\mathbf{r},t)$ is director and can be written as a sum of static part $\mathbf{n}_0(\mathbf{r})$ that describes its equilibrium configuration and small, time-dependent part $\delta\mathbf{n}(\mathbf{r},t)$ that describes the orientational fluctuations around the equilibrium configuration. By knowing the static configuration, i.e., the solution of the Eq. (2) with $\partial/\partial t\mathbf{n}=\mathbf{0}$, one can calculate the eigenmodes of orientational fluctuations by linearization of the Eq. (2) in terms of $\delta\mathbf{n}$,

$$\begin{aligned}&\nabla^2\delta\mathbf{n}-(\mathbf{n}_0\cdot\nabla^2\mathbf{n}_0)\delta\mathbf{n}-(\mathbf{n}_0\cdot\nabla^2\delta\mathbf{n})\mathbf{n}_0\\&-(\delta\mathbf{n}\cdot\nabla^2\mathbf{n}_0)\mathbf{n}_0=-k_N^2\delta\mathbf{n}.\end{aligned} \tag{3}$$

The solutions of Eq. (3) depend on the shape of the cavity and boundary conditions [7],

$$\begin{aligned}&K(\boldsymbol{\nu}\cdot\nabla)\delta\mathbf{n}-W(\mathbf{n}_p\cdot\delta\mathbf{n})\mathbf{n}_p+2W(\mathbf{n}_p\cdot\boldsymbol{n}_0)(\mathbf{n}_p\cdot\delta\mathbf{n})\mathbf{n}_0\\&+W(\mathbf{n}_p\cdot\mathbf{n}_0)^2\delta\mathbf{n}=-\zeta\delta\dot{\mathbf{n}},\end{aligned} \tag{4}$$

where $\boldsymbol{\nu}$ is unit vector normal to the surface, $\mathbf{n}_p$ is the orientation of the director preferred by the surface, W is the surface anchoring strength, and ζ is the surface orientational viscosity.

The most simple one-dimensional confined system, i.e., a nematic layer, has been treated both theoretically [7] and experimentally [10]. It has been shown how anchoring strength affects the relaxation rates of the orientational fluctuations, but the influence of the surface orientational viscosity has not been examined yet. Since this is the system where one can understand physics best, we will review most important results. In a uniform nematic layer placed between two equally treated glass plates the shape of the eigenmode of the orientational fluctuations is $\cos(kz)$ and $\sin(kz)$ for even and odd modes, respectively. The z axis is perpendicular to a nematic layer and $z=0$ lays in the middle of the layer. The layer thickness is d and eigenvalues of the eigenmodes of the orientational fluctuations are denoted by k. In the case of a strong anchoring regime, i.e., the director orientation on the surface does not deviate from the orientation that is preferred by the surface, the amplitude of the orientational fluctuations on the surface is equal to 0, eigenvalues to $k=(N+1)\pi/d$ $(N=0,1,\ldots)$, and the relaxation time depends only on the bulk viscoelastic properties of liquid crystal and the thickness of the layer,

$$\tau=\frac{\eta d^2}{K(N+1)^2\pi^2}. \tag{5}$$

The last expression simply reflects the fact, that due to the fluctuation a deformation of the director appears and therefore an elastic torque appears that forces the director back to its equilibrium orientation. A viscous torque opposes this motion.

In weak anchoring regime the amplitude of the director orientational fluctuations at the surface is not zero, so in addition to the bulk elastic torque also surface elastic torque contributes to the restoring torque on the director. To see how this affects the relaxation times of the orientational fluctuations one has to look at the boundary conditions,

$$\mp K\vartheta'(z,t)-W\vartheta(z,t)=\zeta\dot{\vartheta}(z,t)\big|_{z=\pm d/2}, \tag{6}$$

where ϑ is the angle between the actual orientation of the director and its equilibrium orientation. Equation (6) is simply a balance equation for the torques at the surface. It leads to secular equations for even and odd modes, respectively

$$\frac{kd}{2}\tan\left(\frac{kd}{2}\right)=\frac{d}{2\lambda}-\frac{d\zeta}{2\eta}k^2, \tag{7}$$

$$\frac{kd}{2}\cot\left(\frac{kd}{2}\right)=-\frac{d}{2\lambda}+\frac{d\zeta}{2\eta}k^2 \tag{8}$$

for the k and hence for the relaxation time. The extrapolation length is given by $\lambda=K/W$. We have examined the first three modes. Figure 1 shows how the shape of the modes, i.e., the eigenvalue k, depends on the anchoring strength, if the surface viscosity is small. The deformation of the director throughout the layer is smaller than in the case of the strong anchoring regime, in fact the weaker is the anchoring the smaller is the deformation inside the layer. In the case of the fundamental mode and a very weak anchoring, $\lambda\gg d$, the deformation inside the layer almost vanishes. The higher modes are less affected by the anchoring. From the comparison of the amplitude of the first odd mode for strong anchoring and for infinitely weak anchoring (Fig. 1) one can see that the deformation of the director field inside the layer and therefore the bulk elastic torque (proportional to the derivative of the amplitude) dominates also for the case of the weak anchoring and therefore always gives the main contribution to the relaxation time, i.e., from strong to infinitely weak anchoring the relaxation time changes only by a factor of four.

The effect of the surface viscosity on the eigenvalue of the modes is different than the effect of the anchoring (Fig. 2). Similar to the surface extrapolation length for the anchoring one can define a length $h=\zeta/\eta$ to describe the dissipation at the surface. It affects the eigenvalue k significantly only when $h\gtrsim d$. While the anchoring can change the eigenvalue of the modes only by π/d, the surface viscosity can reduce it by $2\pi/d$ (Fig. 2). This means that not only the relaxation time of the fundamental mode goes to infinity with increasing h, but also the first odd mode. Another interesting feature is that, when $h\gg d$, the second even mode becomes the same as the fundamental mode in the case of the strong anchoring (Fig. 2). The origin of the surface viscosity, however, is not very clear. It can be due to dissipation coming

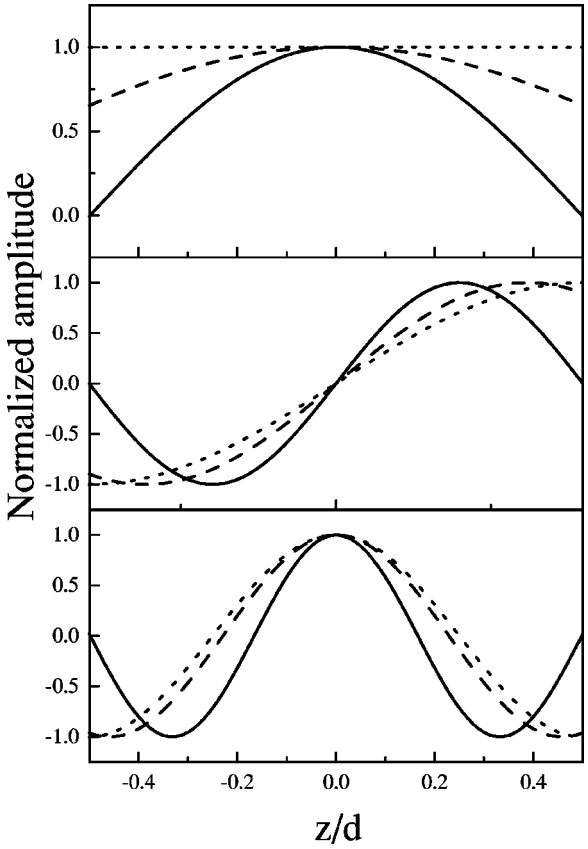

FIG. 1. Calculated normalized amplitude of the first three modes in a nematic layer for different values of anchoring, strong (line), intermediate $\lambda/d=0.5$ (dashed) and weak $\lambda/d=500$ (dots) anchoring. $h/2d=0.001$.

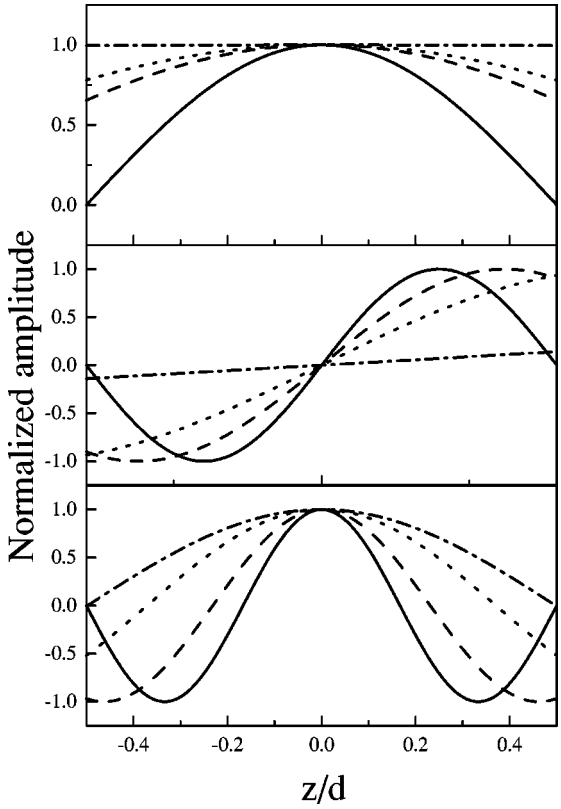

FIG. 2. Calculated normalized amplitude of the first three modes in a nematic layer for different values of the surface viscosity, $h/2d=0.01$(dashed), $h/2d=1$ (dots), $h/2d=100$ (dot-dashed), $\lambda/d=0.5$ in all three cases. Line presents a strong anchoring case.

from surface processes like adsorption desorption or molecular slipping on the surface. What are the possible values for h is an open question.

The mode that can be easily used to measure the properties of the surface interaction is the fundamental mode. For $d\lesssim\lambda$ the secular equation yields approximate solution for the relaxation time of the fundamental mode

$$\tau\approx\frac{\eta d^2}{12K}+\frac{\eta d}{2W}+\frac{\zeta}{W}. \tag{9}$$

The first term is usual bulk term and it prevails upon the second one when the thickness of the layer is much larger than the surface extrapolation length λ, i.e., in the strong anchoring regime where the relaxation time is given by expression (5). The second term describes the contribution of the surface elastic torque to the relaxation of the director in the layer, while the last term comes from the relaxation of the director at the surface and it does not depend on the thickness of the layer. Numerical examination of the Eq. (7) has shown that the expression (9) is a good approximation also for the layer thicknesses somewhat larger than λ. By measuring the thickness dependence of the relaxation rate of the fundamental mode one can, in principle, obtain both the anchoring strength and the surface viscosity. Experimentally in the layer only the first has been measured [10], however, the thinnest layer measured in those experiments had a thickness of 125 nm. That could indicate that h was smaller than 100 nm. To observe the contribution of the surface orientational viscosity one would probably need to measure the layers of the thicknesses of a few 10 nm and very thin layers are experimentally very difficult to prepare and the intensity of light scattered by a single layer becomes very low.

In other confined systems the situation is more complex, the equilibrium configuration of the director is not uniform and the calculation of the eigenmodes is more involved. The most simple and experimentally accessible confined system in two dimensions is liquid crystal embedded in cylindrical pores of either polycarbonate (Nuclepore) or silica (Anopore) membranes. Also in the cylinder the properties of the fundamental mode are similar to those in the layer. We focus on the liquid crystal embedded in Nuclepore membranes, since those were used in our experiments. The equilibrium configuration of the director field in the pores of Nuclepore membranes is known to be either escaped radial with point defects or, for small anchoring strength, planar polar where the director is in the plane perpendicular to the cylinder axis and nearly perpendicular to the pore walls except at two opposite points on the perimeter [11,12]. In the one elastic constant approximation, the analytic form of static director configuration of the latter is known [12]. From this solution we deduced the linearized equation of the fluctuations in the axial direction u of the static structure in the following form:

$$\nabla^2 u+\frac{4\gamma^2 r^2}{R^4+\gamma^2 r^4-2\gamma^2 R^2 r^2\cos 2\varphi}u=-k^2 u, \tag{10}$$

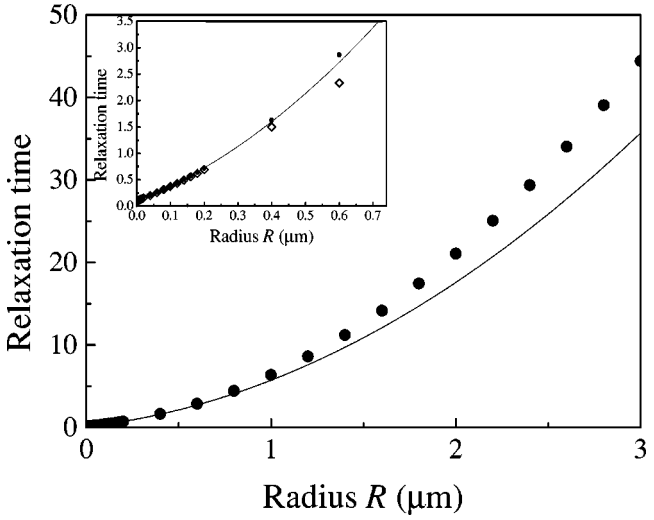

FIG. 3. The dependence of the calculated relaxation time [in the units of $(2\lambda)^2\eta/K$] of the fundamental eigenmode of the director orientational fluctuations on the radius of the cylinder (circles). The line is approximate relaxation time given by expression (13). $\lambda = 100$ nm and $h = 40$ nm. Inset: Comparison of the calculated average relaxation time measured in the scattering experiment at $q = 5/\mu$m (diamonds) and the relaxation time of the fundamental mode (circles).

where φ is the polar coordinate and $\gamma = (\sqrt{4\lambda^2 + R^2} - 2\lambda)/R$. The boundary condition for u reads

$$\left[2(\gamma + \gamma^2 + \gamma^3 \cos 2\varphi)u + r\frac{\partial u}{\partial r} - \frac{r\zeta}{2K}\frac{\partial u}{\partial t}\right]_{r=R} = 0. \quad (11)$$

For $\lambda \gg R$, that is for small anchoring strength, $\gamma = R/4\lambda$, so we may seek an approximate solution to Eqs. (10) and (11) correct to linear terms in γ. This gives us just the standard Helmholtz equation with mixed boundary conditions, so the eigenvalues are given as the solution of the transcendental equation

$$2k_N\lambda J_1(k_N R) = \left(1 - \frac{\zeta}{\eta}\lambda k_N^2\right) J_0(k_N R), \quad (12)$$

where $J_0(k_N R)$ and $J_1(k_N R)$ are Bessel functions of the first kind. Figure 3 shows the dependence of the relaxation time of the fundamental mode on the radius of cylindrical pores numerically calculated from Eq. (12). While for large radii the dependence of its relaxation time on the radius is quadratic, it is linear for small radii. For $\lambda > R$, to calculate the fundamental eigenvalue we can expand the right hand side of Eq. (12) in power series and calculate k_1 to the second order in $1/R$. Using Eq. (1) we then get for the relaxation time of the fundamental mode of the planar structure with weak anchoring

$$\tau_1 \approx \frac{\eta R^2}{8K} + \frac{R\eta}{W} + \frac{\zeta}{W}. \quad (13)$$

The corrections to the relaxation time due to the second term in Eq. (10), which can be obtained by perturbation theory, are proportional to γ^2, so they do not influence the leading terms in Eq. (13). Also, numerical examination of the solutions to Eqs. (10) and (11) shows that this approximation holds reasonably well even when $\lambda \lesssim R$ (Fig. 3). Expression (13) is very similar to the situation in the layer, i.e., expression (9). As in the case of a nematic layer, the second term in Eq. (13) dominates when $\lambda \gtrsim R$ so the orientational fluctuations in this case are governed by surface anchoring and not by bulk orientational elasticity. The contribution of the surface viscosity is the same in both cases.

III. LIGHT SCATTERING

The light is scattered by the inhomogeneities of the dielectric tensor ε. In the dipole far-field approximation and for the processes that are slow compared to the frequency of light ω, the electric field amplitude of the scattered light with the wave vector $\mathbf{k}_f$, and the polarization $\mathbf{f}$ is given by [13]

$$E_s(\mathbf{q},t) = \frac{E_0\omega^2}{4\pi c^2 s}\int_{V_{scatt}} e^{-i\mathbf{q}\cdot\mathbf{r}}[\mathbf{f}\cdot\underline{\varepsilon}(\mathbf{r},t)\cdot\mathbf{i}]d^3\mathbf{r}, \quad (14)$$

where s is the distance between the sample and detector, c the speed of light in vacuum, and $\mathbf{q} = \mathbf{k}_f - \mathbf{k}_i$ the scattering vector. E_0 is the electric field amplitude, $\mathbf{k}_i$ the wave vector, and $\mathbf{i}$ the polarization of the incident light. Dielectric tensor $\underline{\varepsilon}(\mathbf{r},t)$ can be expressed in terms of nematic director, i.e., its dynamic part in the terms of eigenmodes of director orientational fluctuations. When scattering volume V_{scatt} is large compared to the wavelength of light, the integral in expression (14) is a Fourier transform of a given component of the dielectric tensor. So in the bulk nematic, where eigenmodes are plane waves, in the light-scattering experiment at a given scattering vector $\mathbf{q}$ one probes modes with the wave vector equal to the scattering vector. When the size of the scattering volume is comparable to the wavelength of light, the scattering vector need not match any mode wave vector and several modes contribute to scattering. In the case of cylindrical geometry and planar equilibrium configuration of the director the eigenmodes are products of axial $e^{-k_z z}$, polar $e^{-m\varphi}$, and radial parts. The radial parts of the eigenmodes are approximately Bessel functions $J_m(k_N r)$. The contribution of the eigenmode with the eigenvalue k_N to the first-order correlation function (measured in the heterodyne regime of scattering) [13] $\langle E_s^*(\mathbf{q},t)E_s(\mathbf{q},t+\tau)\rangle$, i.e., to the differential scattering cross section of the mode, is then proportional to

$$\left[\frac{\delta(q_\parallel - k_z)}{k_N}\int_0^R J_m(k_N r)J_m(q_\perp r)r\,dr\right]^2, \quad (15)$$

where $q_\parallel$ and $q_\perp$ are the components of the scattering vector parallel and perpendicular to the cylindrical axis, respectively, and k_z the eigenvalue of the axial part of the eigenmode. In the following we will discuss modes with zero axial component of the wave vector, $k_z = 0$. If $k_z \neq 0$, it only contributes a term $K/\eta k_z^2$ to the relaxation rate of the modes.

Figure 4 shows calculated differential scattering cross sections for the first four modes vs scattering vector. The scattering from the fundamental mode strongly prevails over the contributions of the other modes for large range of values of qR. That means that in the scattering experiment one measures mostly the fundamental mode up to scattering vectors a few times larger than $1/R$.

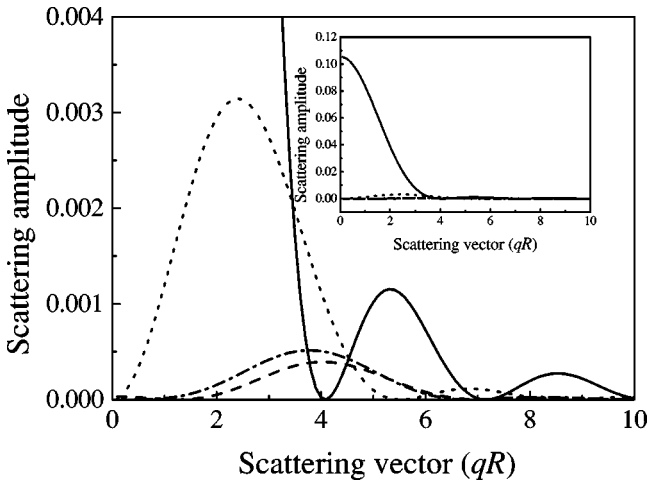

FIG. 4. The differential scattering cross section (arb. units) vs scattering vector for the slowest four modes. $\lambda/R=0.5$ and $h/2R=0.001$.

Figure 5 shows the dependence of calculated average relaxation rate vs scattering vector. While in the bulk this dependence is equal to the dependence of the relaxation rate of the orientational fluctuations on the wave vector, the situation in cylindrical geometry is different. For $qR \lesssim 2$, the measured relaxation rate is equal to the relaxation rate of the fundamental mode of director orientational fluctuations. That means that also at the scattering vector equal to the eigenvalue of the second mode the scattering from the fundamental mode prevails. This can also be seen in Fig. 4, where the first peak of the differential cross section of the second mode lays within the peak of the fundamental mode, which is quite different from the selection rules valid for the bulk. While in the bulk the dependence of the measured relaxation rate vs scattering vector gives the ratio K/η, obviously this is not the case in cylinders. On the other hand, expression (13) shows that this information can be obtained by measuring the dependence of the relaxation rate on the radius.

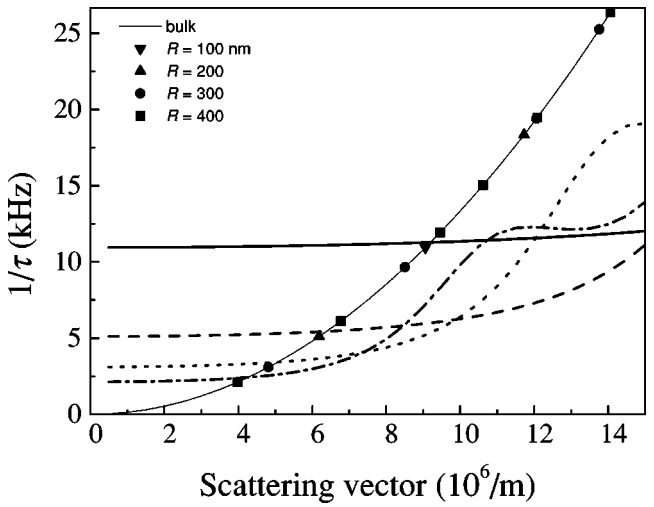

FIG. 5. The dependence of calculated measured relaxation rate vs scattering vector for different radii, $R=100$ nm (solid line), $R=200$ nm (dashed), $R=300$ nm (dot), and $R=400$ nm (dot-dashed) The relaxation rates of the eigenmodes of director orientational fluctuations for different radii are also plotted for comparison. Thin line presents the bulk case. $\lambda=100$ nm and $h=10$ nm.

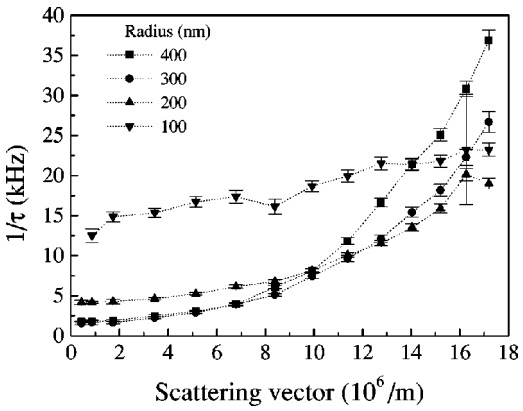

FIG. 6. The relaxation rate of the orientational fluctuations vs the scattering vector. The scattering vector is perpendicular to the axis of the cylindrical pores. Dots are guides to the eye. ($T=295$ K).

The situation is similar in all confined systems. At a given scattering vector one always measures contribution of several modes. How much a given mode contributes depends on how well it is coupled with a plane wave $e^{-\mathbf{q}\cdot\mathbf{r}}$. In the layer, for example, the contribution of the fundamental mode to the scattering is also significant up to scattering vectors that are equal to the wave vectors of a few next modes, but when the scattering vector is equal or very close to a wave vector of a given mode the contribution of this mode always prevails [7].

IV. EXPERIMENTS AND DISCUSSION

As shown in the previous sections, well-defined geometric static properties of the nematic liquid crystal embedded in cylindrical pores of the Nuclepore membranes allow us to fully analyze the light scattering data. In the following, we will present results of the DLS experiments performed in this system, of which a brief report has already been given in Ref. [14].

Our samples were prepared similarly as described in Ref. [11]. A piece of membrane was wetted with the liquid crystal 4-pentyl-4'-cyanobiphenyl (5CB) that filled the cylindrical pores of the membrane due to the capillary action. The re-

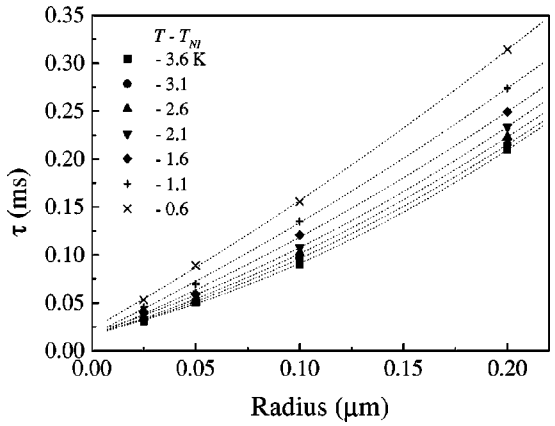

FIG. 7. Dependence of the relaxation rate of the fundamental mode on the cylinder radius at different tempertures. Lines are the second order polynomial fits.

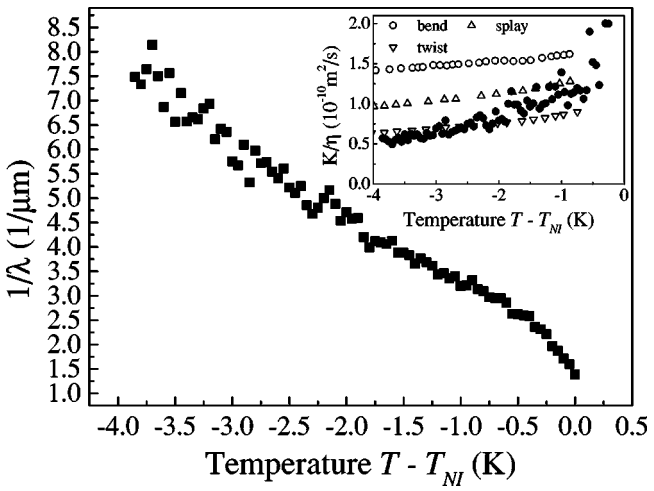

FIG. 8. Temperature dependence of the inverse penetration depth. Inset: comparison of measured diffusivity (full circles) with the diffusivities of pure modes where the backflow is not considered.

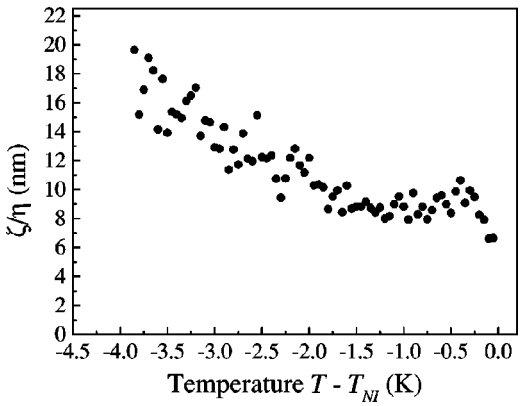

FIG. 9. Temperature dependence of h, i.e., surface to bulk viscosity ζ/η.

maining liquid crystal on the surface of the membrane was removed by pressing the membrane between two Whatman filtration papers and then the filled membrane was placed between two glass plates. The refractive index of the polycarbonate Nuclepore membranes approximately matches the average refractive index of the 5CB, so multiple scattering in the samples was negligible.

The light source was a He-Ne laser with the wavelength of 632.8 nm. The intensity correlation function was measured using an ALV5000 correlator that enables measurements over a time range of $10^{-8}-10^{3}$ s. We have measured the normalized intensity correlation function $g^{(2)}(\tau)=\langle I(t)I(t+\tau)\rangle/\langle I(t)\rangle\langle I(t+\tau)\rangle$ of light exiting the sample as a function of scattering angle, the radius of cavities and the temperature. The incoming and scattered directions were chosen so that the scattering vector was perpendicular to the axis of the pores. Following the selection rules, by which the orientational fluctuations are coupled to the off-diagonal elements of the dielectric tensor, we chose orthogonal polarizations of incident and scattered light.

The measured intensity correlation functions showed a well-defined relaxation component, which is due to the orientational director fluctuations in the pores. The amount of statically scattered light off the sample and pore surfaces was such that the measurements were in the heterodyne regime and the relaxation rate of the intensity correlation function is equal to the relaxation rate of the fluctuations.

Figure 6 shows the dependence of the observed relaxation rate on the scattering vector. Clearly, at small scattering vectors, the relaxation rates become independent of q whereas it increases for $q \gg 1/R$. One should note somehow surprising crossings of the curves for different radii. Such crossings can also be observed in Fig. 5, where theoretical prediction is shown. The position of the crossings of the experimental and theoretical results are in good agreement and the reason for them is the specific shape of the differential scattering cross sections of the modes (Fig. 4).

In Fig. 7, measured relaxation time τ vs R with its fit to Eq. (13) is shown for several temperatures. The coefficient of the linear term, together with the bulk values of K/η, gives the extrapolation length λ, plotted vs T in Fig. 8. The constant term can be used to get h, and it is shown in Fig. 9. The quadratic coefficient, giving the bulk orientational diffusivity K/η, can only be obtained for $T_{NI}-T>0.5$ K and then is quite scattered, but the average value is of the order of 10^{-10} m^2/s, which is close to the known bulk values for 5CB if we assume that backflow does not contribute to the effective viscosity (inset of Fig. 8). The correct value for the quadratic coefficient gives a strong support to our analysis.

The dependence of λ^{-1} on T in Fig. 8 is nearly linear, so that $\lambda^{-1} \propto S^2$, where S is the scalar order parameter. As $K \propto S^2$ [3], and $\lambda = K/W$, $W \propto S^4$. That λ increases as T approaches T_{NI} has also been observed by other authors [15].

Using the known values for K, we get that the surface anchoring strength is 3×10^{-6} J/m^2 close to T_{NI} and 5×10^{-5} J/m^{2}4 K below T_{NI}. At these anchoring strengths the deuterium nuclear magnetic resonance experiments have shown that the configuration of the director is planar polar [12].

Our measured values for h, i.e., the ratio ζ/η, shown in Fig. 9, are in the range of molecular size. This is similar as is obtained for the translational surface friction in ordinary liquids [5]. ζ has also been obtained in rather different conditions in Ref. [16]. There the obtained ratio ζ/η is of the order of extrapolation length, a macroscopic length having nothing to do with dissipation and nearly two orders of magnitude larger than our value. The existence of a surface specific dissipation coefficient has been a matter of some debate [6,16,17]. Durand and Virga [6] presented a model where the surface dissipation comes only from the director rotation and associated backflow close to the boundary.

V. CONCLUSIONS

To conclude, in dynamic light scattering we observed that the orientational fluctuations in small pores are dominated by surface properties. From the measurements we deduce not only the temperature behavior of the surface extrapolation length and surface-anchoring strength W, but also the surface viscosity coefficient. Its ratio to the bulk viscosity is in the range of molecular lengths.

ACKNOWLEDGMENTS

This work was supported by the Ministry of Science and Technology of Slovenia through Grant No. J1-7474 and the European Union through Grant No. IC15-CT96-0744.

[1] Orsay Liquid Crystal Group, Phys. Rev. Lett. **22**, 1361 (1969).
[2] Orsay Liquid Crystal Group, J. Chem. Phys. **51**, 816 (1969).
[3] P. G. de Gennes and J. Prost, *The Physics of Liquid Crystals*, (Clarendon, Oxford, 1993).
[4] For a recent review see G. Barbero and G. Durand, in *Liquid Crystals in Complex Geometries Formed by Polymer and Porous Networks*, edited by G. P. Crawford and S. Žumer (Taylor and Francis, London, 1996) p. 21.
[5] L. Bocquet and J.-L. Barrat, Phys. Rev. Lett. **70**, 2726 (1993).
[6] G. E. Durand and E. G. Virga, Phys. Rev. E **59**, 4137 (1999).
[7] S. Stallinga, M. M. Wittebrood, D. H. Luijendijk, and Th. Rasing, Phys. Rev. E **53**, 6085 (1996).
[8] P. Ziherl and S. Žumer, Phys. Rev. E **54**, 1592 (1996).
[9] J. R. Kelly and P. Palffy-Muhoray, Phys. Rev. E **55**, 4378 (1997).
[10] M. M. Wittebrood, Th. Rasing, S. Stallinga, and I. Muševič, Phys. Rev. Lett. **80**, 1232 (1998).
[11] G. P. Crawford, D. W. Allender, J. W. Doane, M. Vilfan, and I. Vilfan, Phys. Rev. A **44**, 2570 (1991).
[12] D. W. Allender, G. P. Crawford, and J. W. Doane, Phys. Rev. Lett. **67**, 1442 (1991).
[13] B. J. Berne and R. Pecora, *Dynamic Light Scattering* (Wiley, New York, 1976).
[14] A. Mertelj and M. Čopič, Phys. Rev. Lett. **81**, 5844 (1998).
[15] Dai-Shik Seo, Yasufumi Limura, and Shunsuke Kobayashi, Appl. Phys. Lett. **61**, 234 (1992); Takashi Sugiyama, Seiyu Kuniyasu, and Shunsuke Kobayashi, Mol. Cryst. Liq. Cryst. **238**, 1 (1994).
[16] A. G. Petrov, A. Th. Ionescu, C. Versace, and N. Scaramuzza, Liq. Cryst. **19(2)**, 169 (1995).
[17] M. Nobili, R. Barberi, and G. Durand, J. Phys. II **5**, 531 (1995).